JOURNAL OF OPTOELECTRONICS AND ADVANCED MATERIALS Vol. 10, No. 2, February 2008, p. 461 - 469

Compact laser spectrofluorometer for water monitoring campaigns of Southern Italian regions affected by salinization and desertification processes

D. CAPUTO-RAPTI, L. FIORANI[a], A. PALUCCI[a*]
University of Ferrara, Department of Earth Sciences, Via Giuseppe Saragat 1, 44100 Ferrara FE, Italy
[a]ENEA, Laser Applications Section, Via Enrico Fermi 45, 00044 Frascati RM, Italy

A compact laser spectrofluorometer has been developed and employed in the diagnosis of water quality parameters in the frame of the Italian project Integrated Research for Applying new technologies and processes for combating DEsertification (RIADE). The instrument has been designed to be autonomously operated in field campaigns as that conducted in the groundwater-bearing areas of Licata (Southern Italy), affected by high salinity contents induced by the Salso river and by coastal seawater intrusion phenomena. Dissolved (chromophoric dissolved organic matter, tyrosine and tryptophan) and particulate (algae) matter was monitored during the abovementioned field campaign (May 2005) in different wells within the countryside around the Licata area. Measurements of that monitoring activity were therefore compared to: a) the groundwater depth of wells, b) the in situ measurement of chemical-physical parameters (electrical conductivity, pH and temperature) and c) the geochemical composition of the groundwater. The results stress the reduction of water retain due to salt releases in the aquifers. Georeferenced maps of the measured parameters are presented and discussed.

(Received February 11, 2007; accepted February 7, 2008)

Keywords: Ground water, Spectrofluorometer, Desertification, Laser, Chromophoric dissolved organic matter, Algae, Salinity

1. Introduction

Desertification is the degradation of land in arid, semi-arid and dry sub-humid areas and it is primarily affected by human activities and climatic variations [1]. Nowadays, this matter does not refer only to the expansion of existing deserts but it occurs because dryland ecosystems are extremely vulnerable to climate changes, over-exploitation and inappropriate land use. Poverty, political instability, deforestation, overgrazing and bad irrigation practices can all undermine the land's fertility. Over 250 million people are directly affected by desertification. In addition, some one billion people in over one hundred countries are at risk. These people include many of the world's poorest, most marginalized, and politically weak citizens [2,3,4].

Grazing alters vegetation properties, water availability, soil erosion and compaction, carbon cycling and many other ecological processes in drylands. However, these changes are affected by natural sources such as the fire regime, new species imported, climate variability and high salinity deposition. The final scenario is mirrored in vegetation losses, fragmentation of ecosystems and decrease in secondary production [5,6].

The impact of desertification particularly emerges in the European countries outward-facing their coasts in the Mediterranean area. Different are the initiatives funded and supported by the European Union in the frame of research and development projects as DESERTLINKS [7], DISMED [8], DSS-DROUGHT [9], WAM-ME [10], ModMED [11], CLEMDES [12], DesertNet [13], CLIMAGRI [14] and MEDALUS [15], in order to deepen the scientific bases and to develop technological instruments in order to improve the management and protection of water resources and land in the Mediterranean countries. To this respect, Italy is a turning point in these initiatives, with the establishment of the Italian Clearing-House on Desertification [16], intended to support the Italian Committee to Combat Desertification.

In the Italian scenario, the impact of desertification is restricted to the southern regions where the risk is linked to water erosion, strong aggressiveness and intense precipitations and to water and soil salinization. The increased water request from coastal inhabitants and territories for agricultural purposes, exceeding the natural availability, triggers the intrusion of marine water thus supporting the desertification risk, through the process of salinization. Moreover, the slow but constant losses of organic matter content in the soils, strongly affects the soil structure and its water retention capability, thus reflecting the influence of changing crop and soil management practices.

To this respect, the Italian project Integrated Research for Applying new technologies and processes for combating DEsertification (RIADE) [17], supported by MIUR (Italian Ministry of Education, University and Research), in the framework of the National Program 2000-2006, had the main goal to provide forecast models as decision support tools to be employed by public administrations in environmental planning processes. Among the activities carried out in this framework, with contributions from different Italian teams, a task was devoted to develop innovative procedures (e.g., radar data to estimate rain characteristics, laser spectroscopy and isotopic analyses to evaluate soil erosion and underground water dynamics, analysis of historical satellite data to reconstruct vegetation dynamics and map climatologically

relevant variables) in order to highlight monitoring key aspects of desertification processes.

The alluvial plain of the Licata town (Southern Italy, Agrigento Prefecture) have been select for the integrated application of the hydrogeochemical and spectroscopical methods in order to settle on qualitative characteristics of the water resources (Fig. 1). Based on the analysis of the stratigraphic, hydrological, hydrogeological and hydrogeochemical data, we could: i) reconstruct the conceptual hydrogeological model, ii) define the alimentation zone of the unconfined aquifer system, iii) characterize the chemical composition of the water resources and iv) recognize the area with the higher risk of contamination.

Fig. 1. Study area and location of the monitored wells. The area above 50 m of altitude is marked in grey.

Laser Induced Fluorescence (LIF) spectroscopy has been chosen for its intrinsic skills to be employed in real time water quality parameter determinations, with portable instruments, during intensive monitoring campaigns. This technique allows one to perform qualitative and quantitative in situ determination of dissolved (pollutants, humic and fulvic acids) or particulate (phytoplankton) organic matter. To this respect, the Italian National Agency for New Technologies, Energy and the Environment (ENEA) laser remote sensing laboratory has designed and developed a new portable instrument, in order to match the requests of monitoring specifications on relevance sites for RIADE.

In late Spring 2005 (May 22 – 25), a field campaign has been carried out in the Licata area, along the Salso river and in different wells in the neighborhood territory. Distribution maps of the measured parameters as: a) dissolved matter (CDOM, i.e. Chromophoric Dissolved Organic Matter, tyrosine and tryptophan), b) particulate matter (algae), c) groundwater depth and d) electrical conductivity, e) pH and f) temperature, are reported and discussed in term of emerging information on ongoing desertification processes.

2. Hydrogeological setting

The first human record within the Licata territory is as old as Late Neolithic. Due to the numerous sulphur mines occurring within the surrounding region, the Licata harbor represented an important trade centre of the Mediterranean till the end of the XX century. The major hydrographic feature of the region is represented by the Southern Imera river, also called Salso river, that crosses the plain from north to south (Fig. 1). The natural changes of the river bed, its delta area and the nearby coastal sector, have strongly influenced the evolution of the landscape and produced altimetric variations spanning from 0 to 50 m above sea level. In Fig. 1, the occurrence of a palaeoriver bed can be observed east of the present-day one.

The area is largely farmed and almost completely covered by greenhouses, where two productive cycles are carried out every year (Autumn-Winter and Spring-Summer), while cultivations need two-three watering per week [18]. Accordingly, in order to satisfy such a large demand on water resources, several bore-holes have been excavated. These wells are commonly built with stones, of large diameter, up to 5 m and rarely exceed 10 m of depth. They are located both inside and outside greenhouses (Fig. 2) and exploit an unconfined, or locally semiconfined, aquifer developed within the alluvial deposits of the Salso river. This aquifer mainly consists of sandy or silt-sandy lenses, locally as coarse as gravels, generally 1 to 10 m thick and hydraulically interconnected [20].

Fig. 2. Example of monitored wells (inside and outside greenhouses).

The largest contributing source to the aquifer is the infiltration of precipitation (mean annual precipitation of 454 mm 1926-2005 with a range of 206 and 1091 mm) and lateral contributions from the Salso River during the high flow periods. Over the period 1926-2005, the mean annual temperature of the region was 18.1 °C. Based on these climatic parameters and following the climate quality index (CQI) [19] the Licata plain is characterized as semiarid, with a mean aridity value of -49. Indeed, the name Salso means "salty", suggesting that there has been a historical awareness of the high salinity in the region. This perception is also clearly supported by the measurement of electrical conductivity (EC) values of 2 to 14 mS/cm (at 20 °C) [0]. These high EC values are the result of the drainage area containing the Messinian evaporitic deposits (the so-called "gessososolfifera" formation [21]).

The measurements of the depth-to-water during May 2005 show variations between 0.5 and 7 m (Fig. 3). In particular, the higher depth-to-water values are observed within the central sector of the plain, while the lower ones were measured in the northwestern sector of the plain and east of Licata. The measured values are due to the combined effect of both the lithological and geometric characteristics of the aquifer and the amount of pumping. The contribution of pumping is likely to be minimal because the measurements have been carried out in wells that were not exploited for one day and therefore the aquifer could be considered in stable conditions. The only exception is represented by the bore-hole located west of “Contrada Molacotogno”, where the measurements were performed with the aquifer in semi-static conditions.

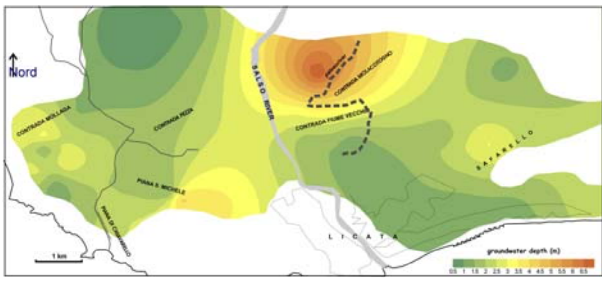

Fig. 3. Spatial distribution of the depth-to-water (m) of the underground water resources in the Licata plain during May 2005 (for the location of the monitored wells see Fig. 1).

Due to the low depth-to-water of the aquifer, the temperature shows strong daily variations with values ranging between 19 and 24.5 °C (Fig. 4). Accordingly, and especially in the large diameter wells, the temperature measurements were made in wells that were not exploited for one day and therefore the aquifer could be considered stable. In particular, the measured values depend on: i) the temperature of the atmosphere, ii) the location of the well inside or outside the greenhouse and iii) the existence of wood-made structures sometimes covering the well. Moreover, the latter two factors influence also the growth of algae in the superficial water.

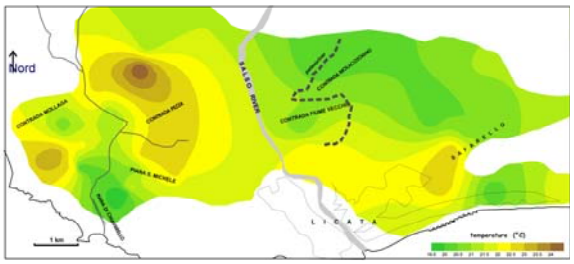

Fig. 4. Spatial distribution of the temperature (°C) of the underground water resources in the Licata plain during May 2005 (for the location of the monitored wells see Fig. 1).

The electrical conductivity of the water (measured in situ at 20 °C) shows variations between 1 and 12 mS/cm (Fig. 5). The minimum values of this parameter are observed in the central and western sectors of the plain, while the highest values measured east of Licata are likely due to the intrusion of saline sea water.

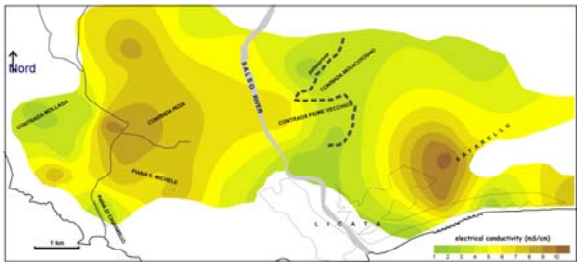

Fig. 5. Spatial distribution of the electrical conductivity (mS/cm at 20 °C) of the underground water resources in the Licata plain during May 2005 (for the location of the monitored wells see Fig. 1).

The mixing phenomena between the freshwater from the aquifer and the saline water are confirmed by elevated concentrations in chlorides up to 4000 mg/l and sodium concentrations greater than 1500 mg/l. Furthermore, the high values of electrical conductivity observed in the plain are caused by diffuse polluting phenomena from nitrates, sulphates and some trace elements, like As, Co, Ni and Cu. The local pollution is primarily associated with the intense farming activities and secondarily with the chemical composition of the sediments hosting the aquifer [20].

Eventually, the combined effect of: i) semi-arid conditions, ii) qualitative deterioration of the underground water resources, iii) high salinity of the Salso river water and iv) occurrence of intense farming activities, renders the Licata plain at high risk of desertification.

3. Compact laser spectrofluorometer

The preliminary sampling and analysis field campaign, carried out in October 2003 in the Licata area with our mobile ENVILAB laboratory, pointed out difficulties to be overcome and protocols to be followed in the design and development of the new portable

instrument [23,24]. A large content of inorganic sediment was the major question to be solved with successive filtration stages before introducing the water sample inside the cuvette for the laser analysis. Furthermore, being the sites to be investigated nearby a dense populated area, affected by anthropic releases, dissolved organic matter (CDOM), protein-like substances (tyrosine, tryptophan, essudate) and pollutants (oils, poly aromatic hydrocarbons, etc.) have to be detected. All these substances are better excited by UV (Ultra Violet) light. On the contrary, organic particles (algae), because of their content of fluorescent pigments as carotenoids, phycocyanin, phycoerythrin and chlorophyll-a, have relevant absorption bands in the blue region of the spectrum. Therefore, two laser sources were employed to match UV and visible excitation wavelengths, and two sample cells in order to improve the discrimination between dissolved and particulated organic substances. Two sources "at the cutting edge" were chosen: a sealed miniaturized frequency-quadrupled Nd:YAG laser (266 nm) and a diode laser (405 nm).

A block diagram of the compact laser spectrofluorometer is given in Fig. 6. Initially, the water sample undergoes a gross filtration ($F_1 = 500$ µm) before entering the hydrodynamic circuit, controlled by the first valve (R_1). The overpressure detector (VS) manages the water flux induced by the pump (P). The second valve (R_2), in open position, allows the water flux to fill the first quartz cuvette (CF_1) or to evacuate the sample. Before the second filtration ($F_2 = 30$ µm), the water pressure is controlled by the detector FL_1 and finally the sample is routed inside the first cuvette for the LIF investigation. At this stage, both dissolved and particulated matter can be inside the water sample. At the exit of the first cuvette, the sample can be evacuated (R_3) or transferred to the last filtration to ($F_3 = 0.2$ µm) at the ending section of the hydraulic circuit. The water flux is controlled by the detector FL_2. The last filter removes all particulate (inorganic and organic): only the dissolved components are introduced in the second cuvette (CF_2) where the sample undergoes the last fluorescence analysis before being evacuated. A beam combiner (BC) allows the overlap of the two laser beams along the same optical path passing through the two analysis cells. The fluorescence emission perpendicular to the beam is colleted by two fiber optics (FO) and transmitted to the respective spectrometers. Two beam shutters (BS) are employed to intercept the laser beams. More details of the optical, hydraulic and electronic components are listed in Table 1.

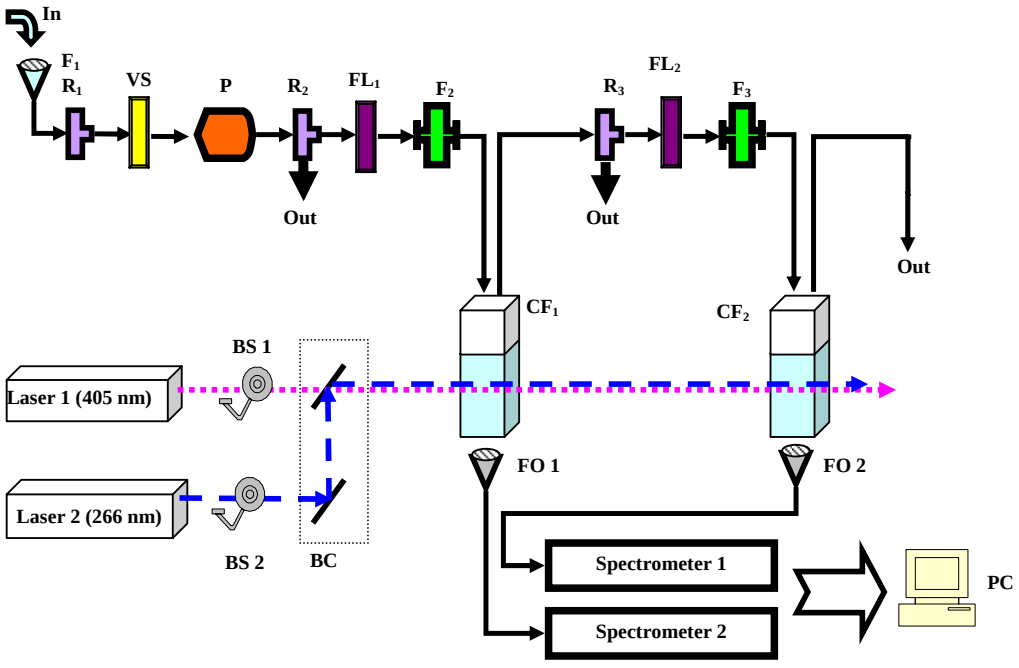

Fig. 6. Layout of the compact laser spectrofluorometer. Optical elements: lasers 1 & 2; beam shutters (BS1, BS2); beam combiner (BC); fiber optics (FO1, FO2); spectrometers 1 & 2. Hydraulic elements: filters (F_1, F_2, F_3); valves (R_1, R_2, R_3); overpressure detector (VS); pump (P); flux detectors (FL_1, FL_2); quartz cuvettes (CF_1, CF_2).

Table 1. Characteristics of the compact laser spectrofluorometer.

Laser 1	JDS Uniphase MicroChip	Nd:YAG IV Harmonic Diode
	λ_{em}	266 nm
	Power	> 2 mW
	Pulse length	600 ps
	Pulse repetition rate	6 KHz
	Stability	< ± 5%
	Polarization	≥ 100:1
Laser 2	Blue Sky Research	Chromalase
	λ_{em}	405 nm
	Power	25 mW
	Noise	≤ 0.5%
	Polarization	≥ 100:1
Spectrometer	Ocean Optics	USB2000
	N° 2	2048 linear CCD array
	Range	200 – 1100 nm
	Sensitivity	86 photons/count
	Integration	3 ms to 60 s - 1 MHZ A/D card
Optical Fiber	N° 2 SMA 905	Single strand, 0.22 NA
Flow Cell	N°2 SELMA	Quartz, 1×1×5 cm^3

The apparatus management is accomplished by an ad-hoc microcontroller electronic module, through a VisualBasic application, and allows the control of all the instrumental settings, i.e. hydraulic circuit switches and laser power supplies through a RS-232 interface connected with the portable computer (PC). Conversely, the USB ports of the portable computer are employed for the two spectrometers, controlled by means of OceanOptics software tools [25].

The compact laser spectrofluorometer is has been conceived for field campaigns: it is battery operated, fully controlled by a portable computer and one measurement takes less than one minute. A view of the final prototype is shown in Fig. 7.

Fig. 7. Picture of the compact laser spectrofluorometer during laboratory tests.

The linear responsivity of the apparatus was tested measuring, in a sample of Milli-Q water, the Raman scattering signal at 292 nm and 460 nm (corresponding to the excitations at 266 nm and 405 nm, respectively) vs the laser intensity (Fig. 8, Table 2). The correlation coefficient of the linear fits ($R^2 > 0.99$) confirm, in both cases, the linearity response of the system.

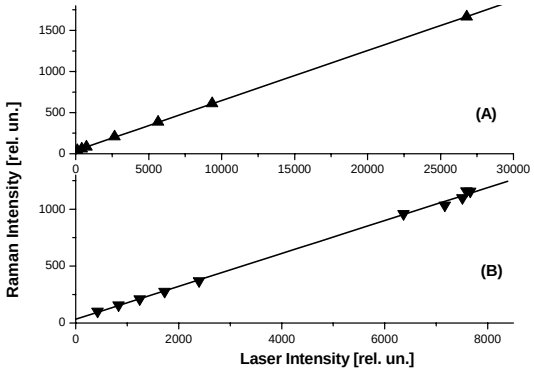

Fig. 8. Linearity tests: water Raman scattering signal vs laser intensity: A) λ_{exc} = 266 nm, λ_{Raman} = 290 nm; B) λ_{exc} = 405 nm, λ_{Raman} = 460 nm.

Table 2. Observed spectral bands (λ_{em}) at different laser excitation wavelengths (λ_{exc}).

Components	**λ_{exc} [nm]**	**λ_{em} [nm]**
Water (Raman scattering)	266	292
Tyrosine	266	315
Tryptophan	266	350
Hydrocarbons	266	420
CDOM	266	450
Phycoerythrin	405	580
Phycocyanin	405	630
Chl-a	405	680

The compact laser fluorometer was calibrated, before the campaign, with standard solutions provided by Sigma-Aldrich: C-5753, i.e. Chlorophyll-a (Chl-a) in methanol, C-5878, i.e. Chlorophyll-b (Chl-b) in methanol, and C-53680, i.e. humic acid in Milli-Q water. The coefficients (y = A x + B) and the correlation coefficients of the linear fits are listed in Table 3.

Table 3. Fitting parameters for the linear calibration of the two spectrometers with standard solutions.

Standard	**Spectrometer**	**A**	**B**	**R^2**	**Conc.**
Chl-a	1	0.2954	-0.0214	0.9998	µg/l
	2	0.3199	-0.0259	0.9999	µg/l
Chl-b	1	0.6061	-0.1023	0.9990	µg/l
	2	0.5478	-0.0927	0.9998	µg/l
Humic acid	1	0.4721	-1.0037	0.9938	mg/l
	2	0.6138	-1.3332	0.9934	mg/l

The data analysis protocol includes a list of steps to be followed before final data release. They can be summarized as follows:

- Subtraction of the electronic and light backgrounds from the fluorescence spectrum.
- Lorentzian fit of the peaks of the spectum.
- Calculation of the integral of the spectrum at some preselected bands, corresponding to the emission of relevant substances (e.g. centered at 680 nm for Chl-a) within a fixed bandwidth (usually 10 nm).
- Subtraction of the spectral background from the integral at the preselected bands (e.g. subtraction of the tail of the CDOM peak from the Chl-a band).
- Preliminary release of the substance concentrations in Raman units, i.e. rationing the integral at the preselected bands to the integral of the Raman peak.
- Final release of the substance concentrations in absolute units (e.g. mg m^{-3}) by calibration with standard solutions.

Time, latitude, longitude and altitude of the sampled site were stored together with spectroscopic information for a further elaboration.

4. Results and discussion

Dissolved organic matter is mainly made of humic and fulvic acids, amino acid proteins, arising from plant and animal (bacteria) life dispersed in the terrains, algal poly-saccharine essudate, phenols. As a consequence, it is linked to biological activity [26,27]. Exhausts or drainages from human activities can strongly contribute to increase the content of CDOM dispersed in inland waters. Moreover, it has been observed that, in case of high salinity rivers [0], CDOM is linked to:

- Total organic content and pCO_2 decrease.
- Chl-a decrease

In the list of chemical substances to be monitored by means of LIF, we can also include protein like compounds, as tyrosine and tryptophan, because they are linked to the biological activity in natural waters. It should be noted also that some inorganic salts, as UO^{2+} and Mn^{2+}, can contribute to the fluorescent emission [29,30].

Intensity and shape of the fluorescence spectrum emitted dissolved organic compounds under study can be affected by different factors:

- pH. Several researchers have observed spectral fluorescence changes either in intensity and position of the emitted bands due to pH increase [31,27]. In particular, variation in acidity modify the spectral shape of the emission by acid functional groups (phenols and phthalate) as well as the conformation of organic molecules.
- Ion-metal interaction. A fluorescence quenching effects due to the ion-metal interaction in humic and fulvic compounds has been described in literature [32].
- Climate. Humic releases in the soils increase with temperature, therefore climate changes can affect the humication contribution on different scales, ranging from short (few years) to very long (hundred years) time scales [33].

The analysis of the signals collected by the compact laser spectrofluorometer allows retrieval of information on both dissolved and particulated organic compounds. To this respect, algal pigments can be disentangled observing the signal at some assigned spectral bands. Nevertheless, CDOM and carotenoids fluorescence could contribute to this signal [34] and, in order to avoid an overestimation of the algal pigments, this effect has to be taken into account with a subtraction of the spectral background.

The sampling procedure in the Licata territory foresaw the installation of the portable spectrofluorometer close to the bore holes and the water spilled and suddenly analysed by the instrument.

The data collected in the Licata territory have been processed after implementation of the protocol described above. Firstly, it has to be mentioned the effectiveness of the double filtration in the discrimination between the fluorescence contributions of particulated and dissolved matter (Fig. 9). In particular, the CDOM fluorescence remains unchanged, while the Chl-a peak disappears after the second filtration (0.2 μm). This procedure allows to precisely disentangle these two contributions: in the final data analysis, the algal content has been obtained from spectra after the first filtration (30 μm), while the dissolved organic matter contribution (tyrosine, tryptophan and CDOM) has been retrieved from spectra after the second filtration (0.2 μm), in order to avoid mutual interferences.

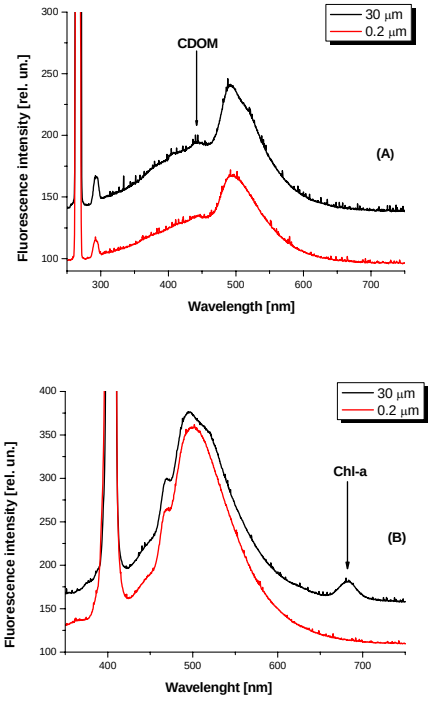

Fig. 9. Fluorescence spectra obtained after the first (30 μm) and second (0.2 μm) filtration: A) Sal5 sample, λ_{exc}=266 nm; B) Sal3 sample, λ_{exc}=405 nm.

Concentrations (CDOM, Chl-a) and fluorescence intensities (tyrosine, tryptophan) collected with the compact laser spectrofluorometer in the groundwater wells of the Licata plain are shown in Fig. 10. The presence of hydrocarbon releases was not detected in the area under study.

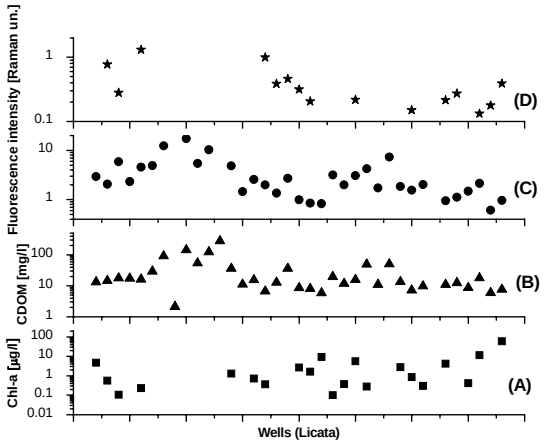

Fig. 10. Concentration and fluorescence intensity distribution of: A) Chl-a; B) CDOM; C) tryptophan and D) tyrosine as measured in the groundwater wells of the Licata territory [May 2005].

High concentrations of organic matter have been monitored in the ground waters, mainly due to the typology of the wells that are open and often completely covered by greenhouses, so that stagnation and high temperatures favor the growth of organic matter.

The monitoring region is strongly affected by the infiltration characteristics of the surrounding land. Fig. 11 and Fig. 12 show the CDOM and Chl-a distribution in the Licata plain. CDOM maxima are present in Contrada Molarga, Contrada Fiume Vecchio and Contrada Saffarello. In the case of Chl-a, also Piana S. Michele has to be included in the list of high concentration sites.

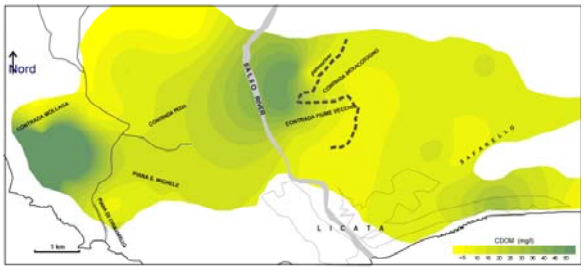

Fig. 11. Spatial distribution of CDOM (mg/l) of the underground water resources in the Licata plain during May 2005 (for the location of the monitored wells see Fig. 1).

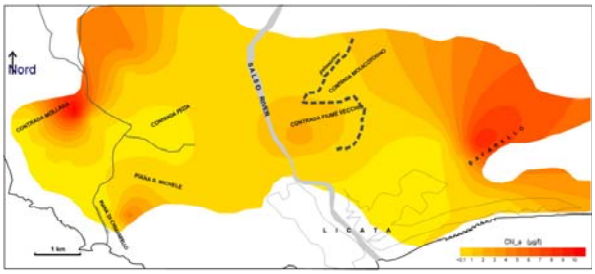

Fig. 12. Spatial distribution of Chl-a (µg/l) of the underground water resources in the Licata plain during May 2005 (for the location of the monitored wells see Fig. 1).

It is well known that Chl-a fluorescence is a good indicator of phytoplankton occurrence in water supplies. The distribution of Chl-a in groundwater of the Licata plain differs by four orders of magnitude among the different wells monitored, exhibiting an exponential decrease with water table depth (Fig. 13, Table 4). The bore-holes belonging to group A are generally located along the border sectors of the plain, while those of group B, which represent a particular area of interest, are located within the central sector of the territory. This area is commonly affected by: i) intrusion phenomena of marine water, similar to the eastern sector of Licata, and ii) lateral infiltration of high salinity water from the Salso river. Intrusion phenomena are mainly due to a lowering of the piezometric level that generates the inversion of the hydraulic gradient and the progressive salinization of the aquifers.

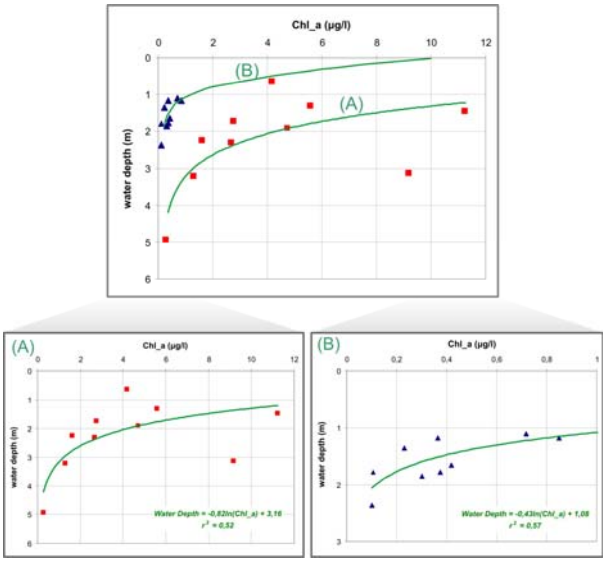

Fig. 13. Chl-a (µg/l) content vs groundwater depth of wells in the Licata area.

Table 4. Fitting parameters for the equation: y = A1 exp(x/t1) + y0 computed for the A and B clusters of data of Fig. 14.

	R^2	y0	A1	t1
A	0.56	1.0152	1.3429	-0.3679
B	0.76	1.7035	4.4068	-0.9442

This study shows that salt intrusion in the aquifer, either from the Salso river or from sea-water, strongly affect the dissolved organic matter content (Fig. 15), especially in the wells of group B, thus reducing its availability in the terrain and therefore its capability to retain water [26,28]. The same trend has been observed in the case of phytoplankton whose growing factor decreases when the EC of the groundwater rises.

Fig. 14. Spatial distribution of the classes A and B (defined in Fig. 13) of the underground water resources in the Licata plain during May 2005 (for the location of the monitored wells see Fig. 1).

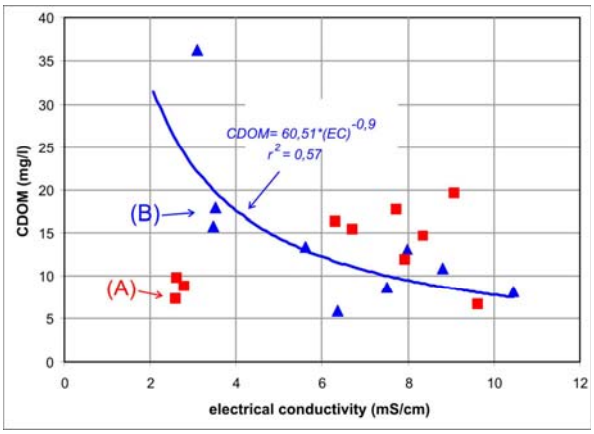

Fig. 15. CDOM (mg/l) content vs electrical conductivity (mS/cm at 20 °C) in the Licata area.

5. Conclusions

A new compact laser spectrofluorometer has been successfully operated during a monitoring campaign in Southern Italy. It demonstrated to be autono`mous, reliable and rugged. Its transportation in the sites to be investigated was easy.

The fluorescence spectra measured by the compact laser spectrofluorometer give information on the chemical composition of the samples.

The data retrieved from the spectral signatures measured by the instrument can supply valuable information for a thorough understanding of the biochemical dynamics of the investigated aquifers and for water classification in real-time monitoring within the framework of the actual regulations. Moreover, the system is able to detect relevant parameters related to desertification processes with high accuracy and sufficient sensibility, and hence to detect seasonal changes.

Acknowledgements

This work has been supported by MIUR – RIADE project. The authors would like to thank the Municipality of Licata and "Assessorato Agricoltura e Foreste" of Licata for the support during the campaign. The contribution of P. Aristipini, R. Giovagnoli and I. Menicucci is kindly acknowledged. The authors are deeply grateful to N. Colonna, M. Iannetta and C. Vaccaro for their involvement.

References

[1] FAO, http://www.fao.org/desertification/
[2] UNCCD (1994) United Nations Convention to combat desertification in those countries experiencing serious drought and/or desertification, particularly in Africa, http://www.unccd.int/
[3] UN (1994) United Nations Earth Summit. Convention on Desertification, United Nations Conference on Environment and Development, Rio de Janeiro, Brazil, 3-14 June 1992, DPI/SD/1576 (New York: United Nations).
[4] EC (1998) Declaration made by the European Community in accordance with article 34(2) and (3) of the United Nations Convention to combat desertification in countries seriously affected by drought and/or desertification, particularly in Africa, http://europa.eu.int/infonet/library/d/convention/en.htm
[5] J. Hill, J. Megier, W. Mehl, Remote Sensing Reviews **12**, 108-130 (1995).
[6] A. J. Ash, D. M. Stafford Smith, N. Abel, (2002) Land degradation and secondary production in semi-arid and arid grazing systems: what is the evidence? In: Global Desertification: Do Humans Cause Deserts? (Reynolds J.F., Stafford Smith D.M., Eds.), pp. 111-134. Dahlem University Press, Berlin.
[7] DESERTLINKS, http://www.kcl.ac.uk/projects/desertlinks/
[8] DISMED, http://dismed.eionet.europa.eu/
[9] DSS-DROUGHT, http://www.medaqua.org/forum/DSS-DROUGHT.html
[10] WAM-ME, http://www.dica.unict.it/users/fvaglias/Wam-meWeb/index.htm
[11] ModMED,

http://homepages.ed.ac.uk/modmed/index.htm
[12] CLEMDES, http://www.inea.it/archivionews.cfm
[13] DesertNet, http://www.desertnet.de/
[14] CLIMAGRI, http://www.climagri.it/
[15] MEDALUS, http://www.medalus.demon.co.uk/
[16] Italian Clearing-House on Desertification, http://www2.minambiente.it/sito/link/siti_ambientali.asp
[17] RIADE, http://www.riade.net/
[18] Regione Siciliana - Assessorato Territorio e Ambiente (2002) Relazione sullo stato dell'ambiente della Sicilia 2002. Suolo e sottosuolo (Palermo: Regione Siciliana).
[19] C. Kosmas, M. Kirkby, N. Geeson, Eds. (1999) Manual on key indicators of desertification and mapping environmentally sensitive areas to desertification, EUR 18882 (Bruxelles: European Commission).
[20] D. Caputo-Rapti, Giornale di Geologia Applicata **2**, 436-444 (2005).
[21] C. Roda, Origine della salinità delle acque del Fiume Salso o Imera Meridionale. Bollettino dell'Accademia Gioenia di Scienze Naturali **10**, 471-530 (1971).
[22] G. P. Asner, K. B. Heidebrecht, Global Change Biology **11**, 182-194 (2005).
[23] P. Aristipini, D. Del Bugaro, L. Fiorani, S. Loreti, A. Palucci (2005) Mobile laser spectrofluorometer for natural waters monitoring in Sicily. Proceedings of SPIE, 5850, 190-195, Advanced Laser Technologies 2004.
[24] Italian Patent N. RM2005A000269 deposed on May 30th 2005.
[25] OceanOptics (2006) OOIBase32™ Spectrometer Operating Software, http://www.oceanoptics.com/Technical/softwaredownloads.asp
[26] P. G. Coble, S. A. Green, N. V. Blough, R. B. Gagosian, Nature **348**, 432-434 (1990).
[27] N. Senesi, T. M. Miano, M. R. Provenzano, G. Brunett, Soil Science **152**, 259-271(1991).
[28] C. D. Clark, W. T. Hiscock, F. J. Millero, G. Hitchcock, L. Brand, W. L. Miller, L. Ziolkowski, R. F. Chen, R. G. Ziza, CDOM distribution and CO_2 production on the Southwest Florida Shelf. Marine Chemistry **89**, 145-167 (2004).
[29] V. A. Pedone, K. R. Cercone, R. C. Burrus, Chemical Geology **88**, 183-190 (1990).
[30] Y. Y. Shopov, D. C. Ford, H. P. Scharcz, Geology **22**, 407-410 (1994).
[31] T. M. Miano, G. Sposito, J. P. Martin, Journal **52**, 1016-1019 (1988).
[32] A. Seritti, E. Morelli, L. Nannicini, A. Giambelluca, G. Scarano, The Science of the Total Environment **148**, 73-81 (1994).
[33] J. Luster, T. Lloyd, G. Sposito, I. V. Fry, Environmental Science and Technology **30**, 1565-1574 (1996).
[34] A. Palucci, Optical and morphological characterization of selected phytoplanktonic communities. In: Optics of Biological Particles (Hoekstra A., Maltsev V., Videen G., Eds.) pp. 165-192. Springer-Verlag, Berlin (2006).
[35] D. Hayashi, W. Hoeben, G. Dooms, Van E. Veldhuizen, W. Rutgers, G. Kroesen, Applied Optics **40**, 986-993 (2001).

*Corresponding author: palucci@frascati.enea.it